

# Molecular-scale Topographic Cues Induce the Orientation and Directional Movement of Fibroblasts on Two-dimensional Collagen Surfaces

Kate Poole<sup>1†\*</sup>, Khaled Khairy<sup>2†</sup>, Jens Friedrichs<sup>1†</sup>, Clemens Franz<sup>1</sup>  
David A. Cisneros<sup>1</sup>, Jonathon Howard<sup>2</sup> and Daniel Mueller<sup>1</sup>

<sup>1</sup>BioTechnological Center  
University of Technology  
Dresden, 01307 Dresden  
Germany

<sup>2</sup>Max Planck Institute for  
Molecular Cell Biology and  
Genetics, 01307 Dresden  
Germany

Collagen fibres within the extracellular matrix lend tensile strength to tissues and form a functional scaffold for cells. Cells can move directionally along the axis of fibrous structures, in a process important in wound healing and cell migration. The precise nature of the structural cues within the collagen fibrils that can direct cell movement are not known. We have investigated the structural features of collagen that are required for directional motility of mouse dermal fibroblasts, by analysing cell movement on two-dimensional collagen surfaces. The surfaces were prepared with aligned fibrils of collagen type I, oriented in a predefined direction. These collagen-coated surfaces were generated with or without the characteristic 67 nm D-periodic banding. Quantitative analysis of cell morphodynamics showed a strong correlation of cell elongation and motional directionality with the orientation of D-periodic collagen microfibrils. Neither directed motility, nor cell body alignment, was observed on aligned collagen lacking D-periodicity, or on D-periodic collagen in the presence of peptide containing an RGD motif. The directional motility of fibroblast cells on aligned collagen type I fibrils cannot be attributed to contact guidance, but requires additional structural information. This allows us to postulate a physiological function for the 67 nm periodicity.

© 2005 Elsevier Ltd. All rights reserved.

\*Corresponding author

*Keywords:* morphodynamics; D-periodicity; fibroblasts; collagen

## Introduction

Collagen is the most abundant protein found in animal connective tissue. Ubiquitous within the extracellular matrix (ECM), collagen acts to maintain the shape and integrity of tissues, and impart tensile strength. The molecular composition and structure of collagen within the ECM varies between different tissues. In tendons and ligaments, bundled, parallel fibrils are aligned in the direction of tension, where the tensile strength is well correlated with the average diameter of the fibre.<sup>1</sup>

In the cornea, collagen fibrils of small diameter form an organized lattice, resulting in a transparent lens capable of resisting external trauma and intraocular pressure.<sup>2–5</sup> Collagen type I is predominantly found in fibrillar form in load-bearing tissues, imparting high tensile strength along the longitudinal axis. Collagen type I molecules are semi-flexible rods of ~300 nm in length and ~1.5 nm diameter, formed from a triple helix of three collagen peptide chains.<sup>6</sup> These collagen molecules assemble into microfibrils, thought to be formed from five molecules, through an entropy-driven process.<sup>7–9</sup> Microfibrils can then form fibrils and the native fibril is characterized by a banding pattern with a period of ~67 nm, known as the D-period. In addition to its role in imparting the mechanical properties of the ECM, collagen acts as a functional scaffold for the cells that inhabit the ECM. Here, we have investigated the influence of structural information within the collagen fibrils on cell alignment, and directional motion of mouse dermal fibroblasts.

† K.P., K.K. and J.F. contributed equally to this work.

Present address: K. Poole, JPK Instruments AG,  
Bouchestrasse 12, 12435 Berlin, Germany.

Abbreviations used: AFM, atomic force microscopy;  
MDF, mouse dermal fibroblast; ECM, extracellular  
matrix.

E-mail address of the corresponding author:  
[poole@jpk.com](mailto:poole@jpk.com)

When presented with aligned components of the ECM, cells can exhibit bi-directional motion, along the axis of fibrous structures.<sup>10</sup> This is presumed important for processes such as wound healing, where contraction of ECM at the wound site by fibroblasts directs the motion of additional cells to the site of the wound. It has been suggested that this directional motion is due to contact guidance. Contact guidance has been demonstrated on a number of artificial, non-biological surfaces,<sup>11–14</sup> with cells aligning in response to physical structures. This led to the hypothesis that cell alignment within three-dimensional gels of oriented collagen is also due to a similar phenomenon.<sup>10,15</sup> However, it has been shown that cells can respond to the mechanical properties of their environment, elongating in the direction of applied tensile strain,<sup>16–17</sup> suggesting that, in three-dimensional gels, contact guidance alone may not account for cell alignment. Accordingly, in order to investigate, in detail, the structures involved in cell alignment and directed motility it is necessary to present cells with components of the ECM that are aligned and mechanically stable as well. However, this is not easy. One problem is that the cells themselves can reorient the ECM: for example, *in vitro* experiments have shown that fibroblasts embedded in collagen gels are able to realign the collagen fibres.<sup>10,18–21</sup> Another problem is that it is difficult to manipulate the orientation of molecules within a three-dimensional matrix. It is also difficult to non-destructively determine collagen fibril substructure within such a three dimensional gel.

What is the influence of the collagen structure on cellular morphodynamics? In order to separate structural from mechanical cues, we have taken advantage of a new technique that allows us to generate stable and oriented collagen monolayers with and without the 67 nm D-period. Under appropriate conditions of temperature and pH, collagen type I self-assembles as a monolayer of oriented fibrils on a mica surface.<sup>22,23</sup> This provides a mechanism to present cells with fixed, oriented collagen fibrils. Furthermore, by manipulation of the buffer conditions during sample preparation, the precise nature of the oriented fibrils can be controlled, with D-banding being dependent on the presence of potassium ions.<sup>23</sup> These surfaces can be characterized by atomic force microscopy (AFM), under physiological conditions, at high resolution and, subsequently, the movement of the cells can easily be quantified.<sup>24</sup>

## Results

### Collagen structure

We have shown that both D-periodic and non-D-periodic collagen can be aligned on mica surfaces.<sup>22,23</sup> The spacing between collagen fibrils within the monolayer and the thickness of fibrils is variable across samples, with significant changes in

structure, depending on the pH of the deposition buffer.<sup>23</sup> This aligned collagen monolayer can be remodelled with the AFM stylus within the first five hours. After this time, the collagen structures cannot be modified, and increasing force leads to destruction of the monolayer.<sup>22</sup> Accordingly, we generated monolayers of unaligned, non-D-periodic/aligned and D-periodic/aligned collagen and left them overnight before the addition of cells. The structure of the aligned collagen monolayers is shown in Figure 1.

### Cell attachment and elongation

A total of 31 time-lapse experiments were performed, 14 with D-periodic/aligned collagen, seven with non-D-periodic/aligned collagen, five with unaligned collagen and five on mica only.

The fibroblast cells attached to all supports. However, the morphology of attached cells varied, depending on the type of support. Phase contrast images were taken starting two hours after the cells were plated. On the non-aligned collagen and mica surfaces, the cells exhibited either the characteristic “kite” shape, or a more circular morphology (Figure 2(a) and (b)). Two hours after plating, the cells that attached to non-D-periodic/aligned collagen showed a morphology similar to that of cells on non-aligned collagen and mica (Figure 2(c)). The cells attached to the D-periodic/aligned collagen had an elongated morphology within two hours of plating. The elongated cells extended a set of lamellipodia parallel with their axis of elongation and, in most cases, two lamellipodia were extended in opposite directions from the cell body (Figure 2(d)).

### Cell body alignment

The time-average cell body alignments ( $\langle\phi\rangle$ , the orientation of the major axis of an ellipse fitted for maximum overlap with the cell body, in degrees) for the cells in contact with the D-periodic/aligned

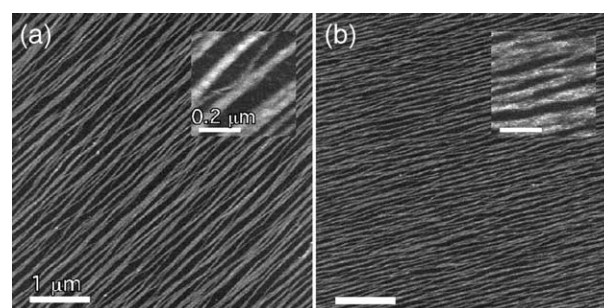


**Figure 1.** Aligned collagen structures with and without D-periodicity. Collagen was aligned in (a) buffer containing potassium, to generate aligned fibrils with D-periodicity (height range: 0–5 nm) or (b) sodium to generate aligned fibrils without D-periodicity (height range: 0–5 nm). The scale bars represent 1  $\mu\text{m}$ , or 200 nm in higher magnification insets.

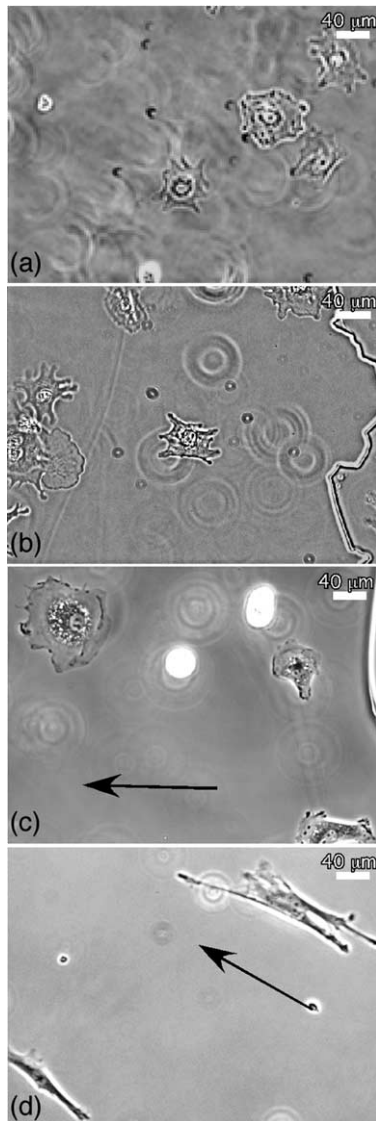


**Figure 2.** The morphology of fibroblast cells is affected by the type of support. Mouse dermal fibroblast cells were plated on mica (a) without collagen, (b) with unaligned collagen, (c) with non-D-periodic/aligned collagen or (d) with D-periodic/aligned collagen, in growth medium containing HEPES and monitored over 16 hours, at 37 °C, with one image taken every two minutes. Only the cells plated on D-periodic/aligned collagen exhibited an elongated morphology over the course of the experiment. Arrows in (c) and (d) indicate the direction of the aligned collagen. The scale bars represent 40  $\mu\text{m}$ .

collagen showed a strong correlation with the angle of collagen orientation,  $\Psi$ . This is seen in the histogram of  $\langle\phi\rangle - \Psi$  (Figure 3(a),  $n=67$ ), which is distributed approximately normally. Student's  $t$ -test confirmed that the mean was not significantly different from zero ( $t(66) = -1.008$ ,  $p > 0.05$ ), indicating that the major axis of the cell is parallel with the substrate orientation. In contrast, in the case of the non-D-periodic/aligned collagen the

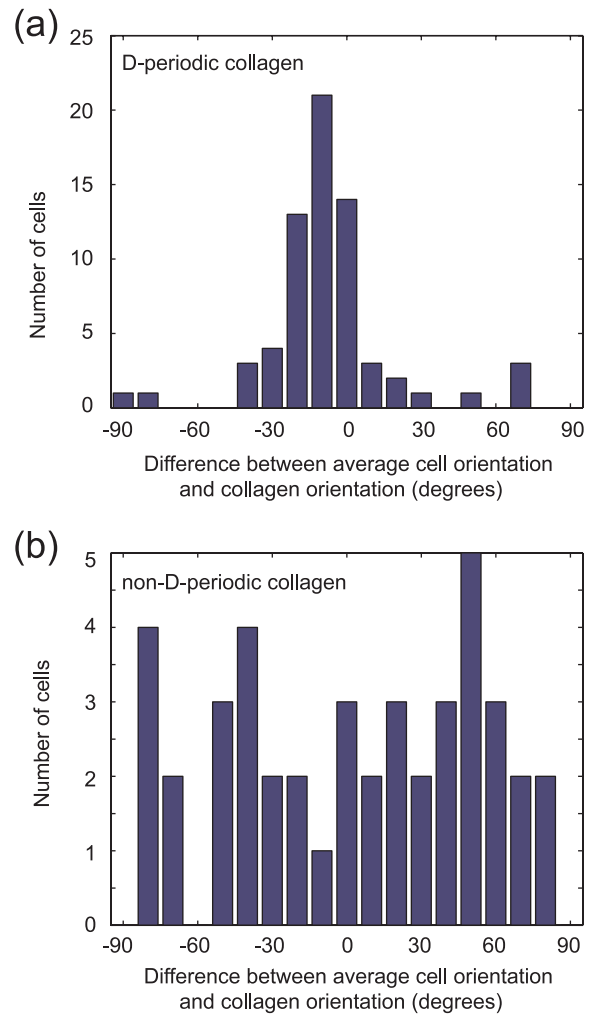


**Figure 3.** The orientation of fibroblasts is influenced by D-periodicity. Histogram analysis of the difference between  $\langle\phi\rangle$  (average orientation of the major axis of the cell) and  $\Psi$  (angle of collagen orientation) for mouse dermal fibroblasts on (a) D-periodic/aligned collagen ( $n=63$ ) and (b) on non-D-periodic/aligned collagen ( $n=43$ ).

histogram was very broad (Figure 3(b),  $n=43$ ), the standard deviation of 51° is close to that expected for uniformly distributed data between  $-90^\circ$  and  $90^\circ$  (52°). These data show that the 67 nm periodicity is necessary for the alignment of fibroblast cells, as this contact guidance is exhibited only on D-periodic, aligned collagen.

### Motility of fibroblast cells

Most cells on the D-periodic/aligned collagen were observed to attach, extend lamellipodia and elongate parallel with the direction of collagen within the first 120 minutes (as stated above and shown in Figure 2). They then moved in the same direction as their long axis. The movement, following elongation of the cell body, involved a quick retraction of the lamellipodia on one side and a

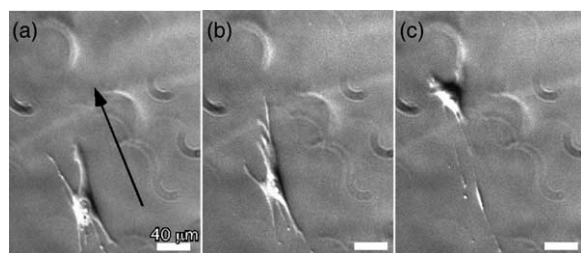


**Figure 4.** Motility of mouse dermal fibroblasts on D-periodic/aligned collagen. Phase contrast, time-lapse pictures of the motion of a typical fibroblast cell on D-periodic/aligned collagen. Images were taken at (a)  $t=120$  minutes, (b) 170 minutes and (c) 220 minutes from plating. The arrow indicates the direction of collagen orientation and the scale bar represents  $40\ \mu\text{m}$ .

large extension on the other. The cell body then became more circular again and the cell slowed for a short period. Such behaviour is shown in Figure 4.

The quantitative motility analysis was conducted as described in Experimental Procedures. Cells that remained alive in the field of view for at least five hours were analysed for their morphology and motility, in order to prevent bias in the selection of cells, and at the same time to ensure that enough position data points could be collected for the motility analysis.

The speed of cell movement was highly variable on each type of surface. Cells on mica have an average speed of  $0.25(\pm 0.15)\ \mu\text{m}\ \text{min}^{-1}$ , on unaligned collagen  $0.34(\pm 0.22)\ \mu\text{m}\ \text{min}^{-1}$ , non-D-periodic/aligned collagen  $0.075(\pm 0.076)\ \mu\text{m}\ \text{min}^{-1}$  and on D-periodic/aligned collagen  $0.81(\pm 0.34)\ \mu\text{m}\ \text{min}^{-1}$  (numbers in parentheses are standard deviations). Motile cells did not exhibit a preferred direction of motion (data not shown) on the mica, unaligned or non-D-periodic/aligned surfaces. However, analysis of the average direction of motion of individual fibroblast cells on D-periodic/aligned collagen, over the course of an experiment, revealed that there is a correlation between the average direction of motion of the cells and the orientation of the D-periodic/aligned collagen microfibrils (Figure 5(a)). Additionally, the average direction of motion of each cell was correlated closely with the average orientation of the major axis (Figure 5(b)).

### Cell orientation in the presence of the RGD peptide

To determine if RGD-mediated integrin binding influences cell body orientation, 3T3 fibroblast cells were added to D-periodic/aligned and non-D-periodic/aligned collagen in the presence or absence of the RGD peptide. An RGD peptide containing a single binding motif was utilized and cell orientation was analysed after one hour. As such, the binding of the RGD peptide by the cell

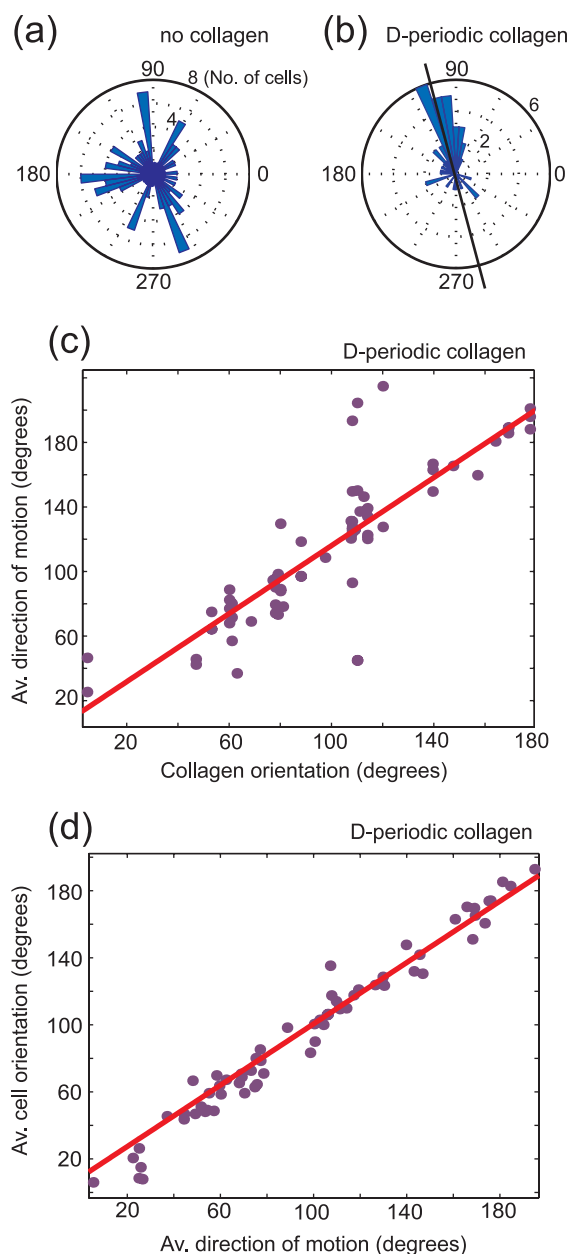


**Figure 5.** Analysis of the directed motility of mouse dermal fibroblasts on D-periodic/aligned collagen. Polar plots of the direction of motion of single cells over the course of an experiment for (a) mica ( $n=112$ ) and (b) D-periodic/aligned collagen ( $n=43$ ,  $\Psi=108$ , indicated by the continuous line), show the random motion on mica only and directed motion on D-periodic/aligned collagen. (c) The average direction of motion of the fibroblasts ( $\theta$ ) is plotted against the angle of orientation of D-periodic collagen ( $\Psi$ ), as determined by AFM ( $n=63$ ). The line fitting gave a correlation coefficient of 0.729. (d) For the same data set, the orientation of the major axis of the cell ( $\phi$ ) was plotted against ( $\theta$ ). In this case the correlation coefficient was 0.831.

surface integrins would not lead to integrin clustering, important for down-stream integrin signalling. Cell binding was not affected on either D-periodic or non-D-periodic substrates in the

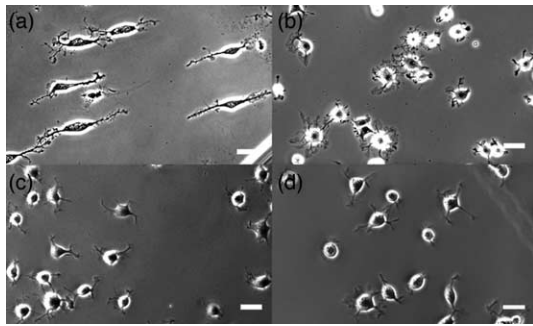


**Figure 6.** The RGD peptide disrupts alignment of Swiss 3T3 fibroblasts on D-periodic/aligned collagen. Phase contrast, time-lapse pictures of fibroblast cell morphology on (a) and (b) D-periodic/aligned and (c) and (d) non-D-periodic/aligned collagen, (a) and (c) in the absence or (b) and (d) in the presence of RGD peptide, taken 60 minutes after plating. The scale bar represents 50  $\mu\text{m}$ .

presence of concentrations of RGD peptide inhibitory to the binding of certain integrins, such as  $\alpha\text{v}\beta\text{3}$  integrin.<sup>25</sup> However, the alignment of the cell body with the orientation of D-periodic collagen fibrils was not observed in the presence of the RGD peptide (Figure 6).

## Discussion

We have shown that two-dimensional monolayers of collagen fibrils can direct the motion of mouse dermal fibroblast cells. The deposition buffers used here were selected because the resulting collagen monolayers exhibited similar density and fibre spacing.<sup>23</sup> However, we confirmed our observations using deposition buffers that generated monolayers of higher collagen density and wider collagen fibrils (data not shown). This supports our hypothesis that it is the D-periodicity of the collagen fibrils that directs cell orientation and motility. Previously, cellular alignment and directed motility has been attributed to contact guidance by longitudinal structures,<sup>10,17</sup> or to mechanosensing of tensile strain by cells.<sup>16–18</sup> However, neither of these mechanisms can account for our results. First, both the D-periodic and non-D-periodic/aligned collagen substrates contain longitudinal structures that should suffice for contact guidance; yet the non-D-periodic substrates did not result in cell alignment and directed motility. And second, both the D-periodic and non-D-periodic/aligned substrates are mechanically stable,<sup>22</sup> are resistant to deformations at AFM forces larger than those generated by cells, and should not be subject to tensile strain by the cells. Yet one induces alignment and the other does not.

In light of the above arguments, we can propose a few alternative mechanisms by which cells respond directionally to D-periodic but not non-D-periodic

collagen. One possibility is that the D-periodicity is functionally important and is recognized by the cells. Perhaps the cellular adhesion apparatus has its own periodicity and that cell orientation and directed motility require alignment of the cellular and acellular structures. It is interesting to note in this respect that the size of two integrin molecules ( $2 \times 8 \text{ nm}$ ) plus two talin adaptors ( $2 \times 8 \text{ nm}$ ) and an actin filament (35 nm) corresponds to the length of the 67 nm D-period. Such an alignment mechanism is consistent with the finding that when integrin-binding sites were separated by  $\geq 73 \text{ nm}$ , cell spreading and attachment were reduced.<sup>26</sup> It cannot be discounted that an extracellular component, such as fibronectin, may bind periodically and act as a linker between the collagen and the cell. However, regardless of whether the information is transmitted through an additional protein, the cell is responding to information contained in the D-periodic nature of the collagen fibrils. Another possibility is that the directional response to the D-periodic/aligned collagen depends on structural cues at the molecular level that are not resolved by the AFM. For example, the D-periodic collagen may present an integrin-binding site that is not presented in the non-D-periodic/aligned substrates. Consistent with this possibility, RGD blocked alignment and directed motility, but not binding, on D-periodic monolayers. This suggests that cells bind to both the periodic and non-periodic substrates through non-RGD dependent integrins,<sup>27</sup> but that the D-periodic substrate presents a cryptic RGD, not presented in the non-D-periodic substrate, that is recognized by an integrin such as  $\alpha\text{v}\beta\text{3}$ .<sup>28</sup> While it could be coincidental that the presentation of RGD is correlated with the appearance of 67 nm periodicity in our AFM images, it is possible that the two are indeed correlated. In other words, the two possibilities may not be mutually exclusive: the D-periodicity could be functionally important, in that it is associated with the presentation of cryptic integrin binding sites.

## Conclusions

The structure of oriented/D-periodic collagen fibrils can determine the direction of alignment and motion of mouse dermal fibroblasts. The directed motion of cells on such a substrate was seen not to depend on mechanosensing, nor solely on the fibrillar nature of the collagen, allowing us to postulate that the 67 nm periodicity observed in collagen fibrils may encode or be associated with structural cues that can direct cellular motion.

## Experimental Procedures

### Preparation of collagen-coated surfaces

Solubilized bovine dermal collagen type I was

purchased from Cohesion (California, USA) and stored at pH 2. For preparation, the collagen was diluted to  $0.3 \mu\text{g ml}^{-1}$ . This solution was flushed over freshly cleaved mica (Mica New York Corp., New York, USA), creating a hydrodynamic flow.<sup>22</sup> To obtain aligned collagen with D-periodicity the collagen was diluted in 50 mM Tris-HCl (pH 7.5), 200 mM NaCl, and left for 15 minutes. The surface was then rinsed and the buffer exchanged for, 50 mM Tris-HCl, (pH 7.5), 200 mM KCl and left at room temperature overnight. For collagen without D-periodicity, collagen was prepared in the absence of potassium ions, but in a buffer containing 200 mM sodium ions,<sup>23</sup> and left overnight. To prepare surfaces coated with unaligned collagen, collagen was diluted in, 50 mM Tris-HCl (pH 3.5), 200 mM KCl, as low pH precludes the formation of aligned collagen microfibrils.<sup>23</sup>

### Cell culture

Primary neonatal mouse dermal fibroblasts (passage 7–14) were maintained in low-glucose DMEM containing 10% (v/v) fetal bovine serum (FBS) and penicillin-streptomycin (all reagents from Gibco-BRL). Routine cultures were fed with fresh medium every second day. To prepare samples for time-lapse video microscopy, cells were released from the plastic using trypsin-EDTA (Invitrogen) and suspended at a concentration of  $5 \times 10^4$  cells  $\text{ml}^{-1}$  in the cell medium described above, with Hepes added. Approximately, 5 ml of the cell suspension was added to a dish with mica/mica + collagen discs glued to the bottom. Cells adhered within 30 minutes. Swiss 3T3 fibroblast cells were maintained in DMEM containing 10% FBS and penicillin-streptomycin (Gibco-BRL). To prepare samples for experiments using the RGD peptide, cells were suspended at a concentration of  $5 \times 10^4$  cells  $\text{ml}^{-1}$  in Hank's buffered salt solution, containing Hepes and added to dishes in the presence (100  $\mu\text{g/ml}$ ) or in the absence of the RGD peptide (GRGDSPK, Sigma).

### Atomic force microscopy

AFM imaging was conducted using a Nanoscope III (Veeco, Santa Barbara, CA) or a NanoWizard (JPK Instruments, Berlin, Germany), mounted on a Zeiss Axiovert 200M (Carl Zeiss, Göttingen, Germany). On the Nanoscope III, topographies were recorded simultaneously in trace and retrace direction, using tapping mode. The  $\text{Si}_3\text{N}_4$  cantilevers used (OMCL TR-400-PS, Olympus, Tokyo) had a resonance peak close to 9 kHz. On the NanoWizard, images were taken in low-force contact mode using 200  $\mu\text{m}$  long V-shaped cantilevers, with nominal spring constants of  $0.06 \text{ N m}^{-1}$ . The force applied to the cantilever was adjusted manually to approximately 50 pN. This force was just sufficient for the stylus of the cantilever to remain in contact with the surface during the scanning process. Images were obtained at a line-scan rate of 1 Hz.

### Time-lapse, phase contrast microscopy

Phase contrast images were obtained using a Zeiss Axiovert 200M inverted microscope (Carl Zeiss, Jena, Germany) with  $20\times$  (NA-0.25) and  $10\times$  (NA-0.4) phase contrast objectives (Carl Zeiss), and a CoolSnap HQ CCD camera (Photometrics, Munich, Germany), driven by Metamorph imaging software (Universal Imaging, Downingtown, USA). Using a motorized stage (Carl Zeiss), each experiment involved tracking 7–12 cells on

1–4 separate mica discs prepared with aligned collagen, unaligned collagen or without collagen, simultaneously, over about 16 hours. Images were collected every two minutes. Time-lapse experiments were conducted at  $37^\circ\text{C}$ , in the cell culture media described above, with Hepes added. For quantitative analysis, the data set was reduced to one outline per cell every ten minutes, which lies within acceptable ranges for rejecting correlated cell positions (see below). Cell outlines were generated manually, as automated and semi-automated software designed for similar edge-detection tasks failed to produce reliable results.

### Cell motility

Cells that remained alive in the field of view for at least five hours were analysed for their morphology and motility, in order to prevent bias in the selection of cells, and at the same time to ensure that enough position data points could be collected for the motility analysis. In some cases, new cells "landed" or entered the field of view after several hours of starting the time-lapse. These were included in the analysis if they satisfied the criteria stated above.

Analysis of the cell motion proceeded by tracking the centroid of the cell over the course of the experiment, generating the corresponding  $x$ - $y$  trajectories. Non-parametric fitting of a smoothing spline piecewise polynomial was applied to the  $x$ - $y$  trajectories and the first derivatives with respect to time,  $\dot{x}_i$  and  $\dot{y}_i$  were evaluated at each time point  $i$ . The average speed  $\langle v \rangle$  is then obtained from:

$$\langle v \rangle = \frac{1}{N} \sum_i^N \sqrt{\dot{x}_i^2 + \dot{y}_i^2}$$

where  $N$  is the size of the original data set. Since the area is obtained from the cell outlines as the number of pixels multiplied by the pixel length squared, we can define a radius  $r$  as the equivalent radius of a circle that has the same area of the cell, and take  $r$  to be the characteristic length scale of our problem such that a correlation time  $\tau$  can be calculated as  $\tau = r/\langle v \rangle$ . The number of independent data points  $n = N(\Delta t/\tau)$ , is then the size of the new vectors  $\dot{x}$  and  $\dot{y}$ . This is equivalent to a resampling of the trajectory for uncorrelated position points, based on  $r$ . In the case of slowly moving cells, this drastically reduces the number of available data points. Cells for which  $n < 10$  over a total period of observation of five hours, were considered non-motile. The vectors  $\dot{x}$  and  $\dot{y}$  are then used in the calculation of the direction of motion  $\theta$  relative to the  $x$ -axis in the image frame:

$$\theta = \tan^{-1}(\dot{y}\dot{x})$$

The distribution of  $\theta$  is fitted to a normal distribution to get the mean direction of orientation of motion  $\langle \theta \rangle$  for an individual cell.

### Cell morphology

For each independent point in the trajectory, an ellipse was fitted to the cell outline to obtain the direction of orientation  $\langle \phi \rangle$  of the major axis of the cell in degrees, relative to the positive  $x$ -axis in the image frame, as well as the ratio of lengths of the minor and the major axes of the fitted ellipse. A distribution over the whole trajectory, as well as average values were also obtained using a fit to a normal distribution.

## Acknowledgements

The authors thank Britta Schroth-Diez for technical assistance. This work was funded by the Volkswagenstiftung, the Free State of Saxony and the European Union.

## References

- Ottani, V., Raspanti, M. & Ruggeri, A. (2001). Collagen structure and functional implications. *Micron*, **32**, 251–260.
- Maurice, D. M. (1957). The structure and transparency of the cornea. *J. Physiol.* **136**, 263–286.
- Boote, C., Dennis, S., Newton, R. H., Puri, H. & Meek, K. M. (2003). Collagen fibrils appear more closely packed in the prepupillary cornea: optical and biomechanical implications. *Invest. Ophthalmol. Vis. Sci.* **44**, 2941–2948.
- Komai, Y. & Ushiki, T. (1991). The three-dimensional organization of collagen fibrils in the human cornea and sclera. *Invest. Ophthalmol. Vis. Sci.* **32**, 2244–2258.
- Meek, K. M., Blamires, T., Elliott, G. F., Gyi, T. J. & Nave, C. (1987). The organisation of collagen fibrils in the human corneal stroma: a synchrotron X-ray diffraction study. *Curr. Eye Res.* **6**, 841–846.
- Kadler, K. E., Holmes, D. F., Trotter, J. A. & Chapman, J. A. (1996). Collagen fibril formation. *Biochem. J.* **316**, 1–11.
- Hulmes, D. J. (2002). Building collagen molecules, fibrils, and suprafibrillar structures. *J. Struct. Biol.* **137**, 2–10.
- Orgel, J. P., Miller, A., Irving, T. C., Fischetti, R. F., Hammersley, A. P. & Wess, T. J. (2001). The *in situ* supermolecular structure of type I collagen. *Structure (Camb)*, **9**, 1061–1069.
- Ottani, V., Martini, D., Franchi, M., Ruggeri, A. & Raspanti, M. (2002). Hierarchical structures in fibrillar collagens. *Micron*, **33**, 587–596.
- Guido, S. & Tranquillo, R. T. (1993). A methodology for the systematic and quantitative study of cell contact guidance in oriented collagen gels. Correlation of fibroblast orientation and gel birefringence. *J. Cell. Sci.* **105**, 317–331.
- Oakley, C., Jaeger, N. A. & Brunette, D. M. (1997). Sensitivity of fibroblasts and their cytoskeletons to substratum topographies: topographic guidance and topographic compensation by micromachined grooves of different dimensions. *Expt. Cell. Res.* **234**, 413–424.
- Walboomers, X. F., Croes, H. J., Ginsel, L. A. & Jansen, J. A. (1998). Growth behavior of fibroblasts on microgrooved polystyrene. *Biomaterials*, **19**, 1861–1868.
- Walboomers, X. F., Ginsel, L. A. & Jansen, J. A. (2000). Early spreading events of fibroblasts on microgrooved substrates. *J. Biomed. Mater. Res.* **51**, 529–534.
- Walboomers, X. F. & Jansen, J. A. (2001). Cell and tissue behavior on micro-grooved surfaces. *Odontology*, **89**, 2–11.
- Oster, G. F., Murray, J. D. & Harris, A. K. (1983). Mechanical aspects of mesenchymal morphogenesis. *J. Embryol. Expt. Morphol.* **78**, 83–125.
- Bischofs, I. B. & Schwarz, U. S. (2003). Cell organization in soft media due to active mechanosensing. *Proc. Natl Acad. Sci. USA*, **100**, 9274–9279.
- Mudera, V. C., Pleass, R., Eastwood, M., Tarnuzzer, R., Schultz, G., Khaw, P. *et al.* (2000). Molecular responses of human dermal fibroblasts to dual cues: contact guidance and mechanical load. *Cell. Motil. Cytoskeleton*, **45**, 1–9.
- Sawhney, R. K. & Howard, J. (2002). Slow local movements of collagen fibers by fibroblasts drive the rapid global self-organization of collagen gels. *J. Cell. Biol.* **157**, 1083–1091.
- L'Heureux, N., Germain, L., Labbe, R. & Auger, F. A. (1993). *In vitro* construction of a human blood vessel from cultured vascular cells: a morphologic study. *J. Vasc. Surg.* **17**, 499–509.
- Klebe, R. J., Caldwell, H. & Milam, S. (1989). Cells transmit spatial information by orienting collagen fibers. *Matrix*, **9**, 451–458.
- Harris, A. K., Stopak, D. & Warner, P. (1984). Generation of spatially periodic patterns by a mechanical instability: a mechanical alternative to the Turing model. *J. Embryol. Expt. Morphol.* **80**, 1–20.
- Jiang, F., Khairy, K., Poole, K., Howard, J. & Muller, D. J. (2004). Creating nanoscopic collagen matrices using atomic force microscopy. *Microsc. Res. Tech.* **64**, 435–440.
- Jiang, F., Horber, H., Howard, J. & Muller, D. J. (2004). Assembly of collagen into microribbons: effects of pH and electrolytes. *J. Struct. Biol.* **148**, 268–278.
- Drake, B., Prater, C. B., Weisenhorn, A. L., Gould, S. A., Albrecht, T. R., Quate, C. F. *et al.* (1989). Imaging crystals, polymers, and processes in water with the atomic force microscope. *Science*, **243**, 1586–1589.
- Kumar, C. C., Malkowski, M., Yin, Z., Tanghetti, E., Yaremko, B., Nechuta, T. *et al.* (2001). Inhibition of angiogenesis and tumor growth by SCH221153, a dual alpha(v)beta3 and alpha(v)beta5 integrin receptor antagonist. *Cancer Res.* **61**, 2232–2238.
- Arnold, M., Cavalcanti-Adam, E. A., Glass, R., Blummel, J., Eck, W., Kantlehner, M. *et al.* (2004). Activation of integrin function by nanopatterned adhesive interfaces. *Chem. Phys. Chem.* **5**, 383–388.
- Gullberg, D., Tingstrom, A., Thureson, A. C., Olsson, L., Terracio, L., Borg, T. K. & Rubin, K. (1990). Beta 1 integrin-mediated collagen gel contraction is stimulated by PDGF. *Expt. Cell. Res.* **186**, 264–272.
- Massia, S. P. & Hubbell, J. A. (1991). An RGD spacing of 440 nm is sufficient for integrin alpha V beta 3-mediated fibroblast spreading and 140 nm for focal contact and stress fiber formation. *J. Cell. Biol.* **114**, 1089–1100.

Edited by W. Baumeister

(Received 22 November 2004; received in revised form 16 March 2005; accepted 23 March 2005)